Hindawi
Advances in Materials Science and Engineering
Volume 2017, Article ID 2676432, 6 pages
https://doi.org/10.1155/2017/2676432

Review Article

Formation and Physical Properties of *h*-BN Atomic Layers: A First-Principles Density-Functional Study

Yoshitaka Fujimoto

Department of Physics, Tokyo Institute of Technology, Tokyo, Japan

Correspondence should be addressed to Yoshitaka Fujimoto; fujimoto@stat.phys.titech.ac.jp

Received 15 June 2017; Accepted 20 July 2017; Published 22 August 2017

Academic Editor: Achim Trampert

Hexagonal boron nitride (*h*-BN) atomic layers have attracted much attention as a potential device material for future nanoelectronics, optoelectronics, and spintronics applications. This review aims to describe the recent works of the first-principles density-functional study on *h*-BN layers. We show physical properties induced by introduction of various kinds of defects in *h*-BN layers. We further discuss the relationship among the defect size, the strain, and the magnetic as well as the electronic properties.

1. Introduction

Since the discovery of a single atomic layer of graphite, that is, graphene, other atomic layers have received much attention [1–8]. Hexagonal boron nitride (*h*-BN) atomic layers, in which alternating boron and nitrogen atoms are arranged on the honeycomb lattices, have also gained a lot of interest because of the similar structural and mechanical properties to graphene [9–11]. On the other hand, electronic properties of *h*-BN layers are considerably different from those of graphene; graphene is a gapless material with metallic conduction [12], and the *h*-BN atomic layers possess a wide band gap [13–15]. Such wide band gap nature of *h*-BN layers is expected to give rise to new physical properties as well as relevant electronic/optoelectronic applications in nanotechnology.

For example, *h*-BN atomic layers exhibit high optical emission intensities in deep ultraviolet (UV) regions [13, 16–18], and the *h*-BN bilayers can transform from an indirect-gap semiconductor to a direct-gap one by applying strains [19]. Thus, *h*-BN layers are highly important optoelectronics device materials used in deep UV lasers and light-emitting diodes [13, 17, 20–23]. The atomic vacancies in *h*-BN layers can be introduced using electron beam irradiations and are shown to be useful as a source of magnetism [10, 24–27]. The introductions of C atoms and graphene-like flakes into *h*-BN sheets have been also performed via electron beam irradiations due to analogous structural properties among B, C, and N elements [28–36], which can tune the electronic and the magnetic properties [37–39]. It is predicted theoretically that the energy band gaps are tunable depending on the size of the graphene flakes [37, 38]. The electronic transport properties of the *h*-BN atomic layers can be changed from insulating to conductive properties when C atoms are doped, suggesting a possibility to fabricate the novel opto/nanoelectronics applications [31, 32, 34–36, 40]. Furthermore, when the C atom is doped, the exotic conduction channel in *h*-BN monolayers would emerge, which might improve electronic transport properties [41–46]. Thus, *h*-BN atomic layers are promising materials to be used in nanoelectronics and optoelectronics applications.

The purpose of this review is to provide the recent progress of the first-principles density-functional calculations that clarify various physical properties of *h*-BN atomic layers with lattice defects including atomic vacancies and carbon defects. In Section 2, the magnetic properties of atomic vacancies in *h*-BN layer are discussed. Section 3 is devoted to discussions on the electronic properties of carbon-doped *h*-BN layers. In Section 4, the behaviors of the magnetic properties and the energy band gaps are shown with the variation of the graphene-like defect size. Finally, Section 5 summarizes this paper together with outlook.

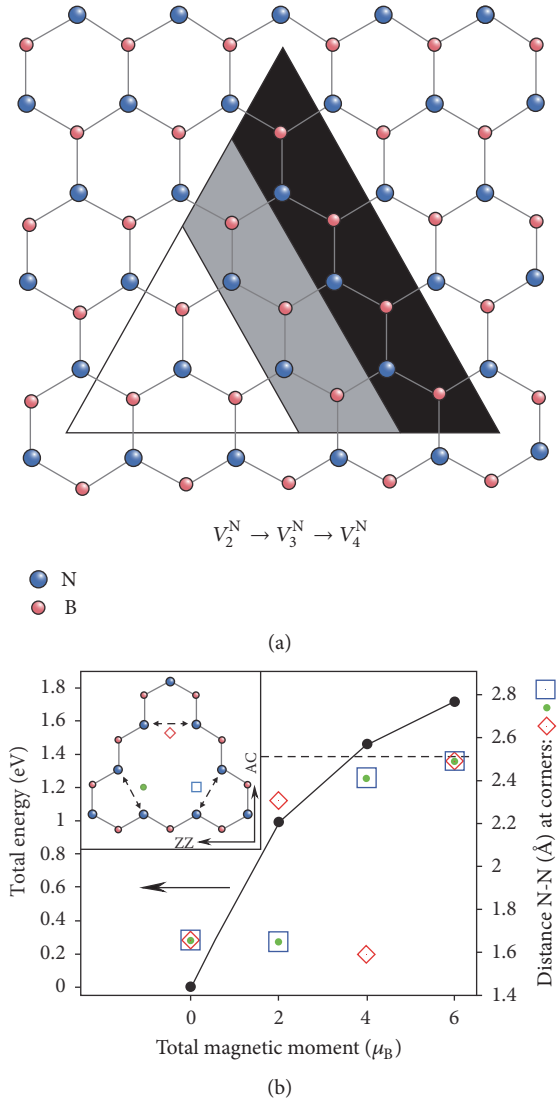

FIGURE 1: (a) Schematic view of h-BN monolayers for atomic vacancies. (b) Total energy and N-N distance near V_2^N defect as a function of imposed magnetic moment. Reproduced with permission from [24]; copyright 2012, the American Institute of Physics.

2. Atomic Vacancy

Atomic vacancies in h-BN layers can be created by electron beam irradiation [10, 25–27]. Triangular-shaped vacancies are observed experimentally by using high-resolution transmission electron microscopy and these vacancies in h-BN layers are arranged with various sizes and peculiar orientation [10]. It is therefore surmised that the B atoms are removed more easily than the N atoms from h-BN monolayers by electron beam irradiation [10].

The introductions of the atomic vacancies into the h-BN monolayers are reported to give rise to the magnetic moment [24, 47]. In Figure 1(a), the schematic view of the triangular atomic vacancies in the h-BN monolayer is shown, where the multivacancies V_T are defined with $T = \sqrt{n_B + n_N}$ and n_B and n_N are the numbers of removed B and N atoms, respectively. The total magnetic moments of V_1^N, V_2^N, and V_3^N are calculated to be 1, 0, and $3\mu_B$, respectively. Unlike graphene [48], the behavior of vacancies V_T^N in the magnetic properties does not follow Lieb's theorem because of the structural reconstructions with the N-N bond formation [49]. When the N-N bond formation is broken, the total magnetic moment increases. The total magnetic moment of the V_2^N defect increases as the N-N distance around the vacancy increases, though the ground state of V_2^N exhibits zero magnetic moment (see Figure 1(b)).

3. Carbon Impurity

Substitutional carbon doping to h-BN layers and BN nanotubes has been performed using the electron beam irradiation technique [32, 33] and substitutionally doped C atoms in the h-BN monolayers have been observed via a transmission electron microscopy method [31]. It was found that the substitution with C atoms decomposed from hydrocarbon molecules takes place mostly at B atom sites, and it was surmised that the substitutional doping proceeds by repairing the B atom vacancies with C atoms broken by the knock-on electron beam [32, 34].

Recent first-principles calculations showed that the substitution of B atoms with C atoms needs less energy costs than that of N atoms under N-rich conditions. Moreover, it was shown that positive charging favors the substitution of B atom with C atom (C_B), whereas negative charging favors the substitution of N atom with C atom (C_N). In addition, it was shown that the substitution of B atom with C atoms may predominately take place even under B-rich conditions [34, 35].

It was reported that the electronic transport properties of h-BN layers can transform from insulating to conductive properties when C atom is doped [32]. The donor-like impurity states appear below the conduction-band minimum (CBM) when C atom is doped at B atom site, whereas the substitution of N atom with C atom gives rise to the acceptor-like impurity states above the valence-band maximum (VBM) [35, 41]. It was shown that ionization energies for acceptor-like as well as donor-like states can be controlled by applying strains (see Figure 2(a)) [41]. The strains can often produce not only the new structural properties but also the novel electronic properties [19, 50, 51]. Interestingly, in the case of the h-BN monolayers, the exotic transport channel will behave as an active state under more than ~1% compressive strains (Figure 2(b)). In addition, the band gaps are also tunable under strains [52–54].

Scanning tunneling microscopy (STM) measurements are one of the effective tools to observe the surface electronic structures at atomic level [55–61]. The B atoms and N atoms in graphene can be clearly identified experimentally and theoretically [62–66]. The STM image of the h-BN monolayer has a large bright triangular shape around the C defect surrounded by six bright spots above each N atom, since the C defect state consists of the triangular-shaped spatial distributions of local density of states (LDOS), and in addition to this defect state, the π states in the valence bands

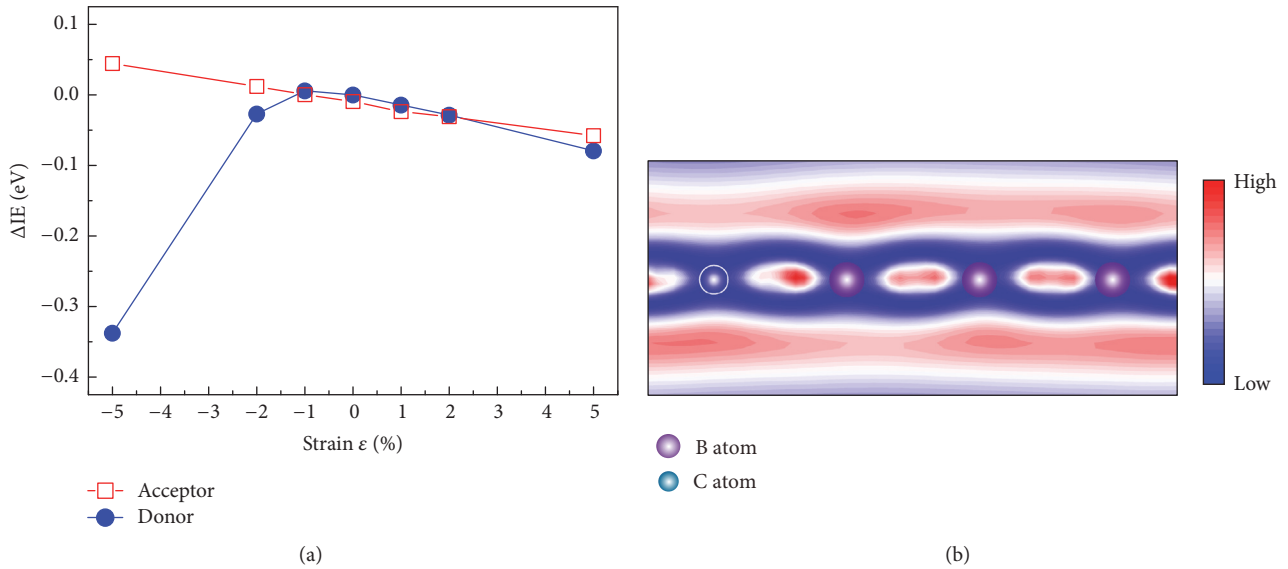

Figure 2: (a) Relative ionization energy (ΔIE) for acceptor and donor states in C-doped h-BN monolayers as a function of applied strain. (b) Contour plot of electron density of C-doped h-BN monolayer at the Γ point of the CBM, where B atom is replaced by C atom. Reproduced with permission from [41]; copyright 2016, the American Physical Society.

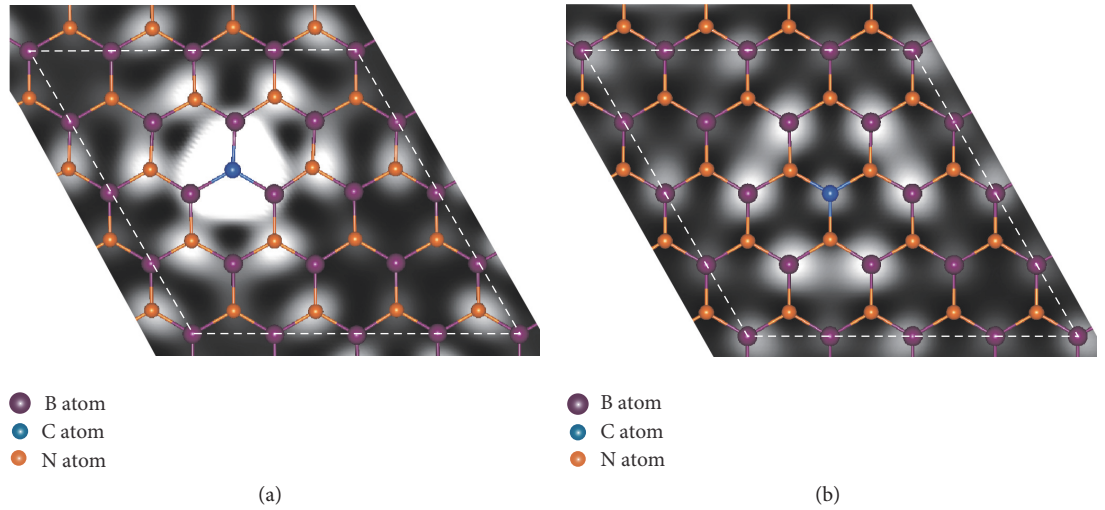

Figure 3: Calculated STM images of C-doped h-BN monolayers, where C atom is replaced at (a) the N site and (b) the B site. Reproduced with permission from [41]; copyright 2016, the American Physical Society.

contribute the STM image (Figure 3(a)). On the other hand, for the C substitution of the B atom, the STM image has a small dark spot above the C defect which is surrounded by six bright spots above each B atom (Figure 3(b)) [41]. The C defects in the h-BN monolayers might be identified by using STM methods.

4. Carbon Flake

The h-BN monolayers embedded with triangular graphene flakes can modify the electronic properties as well as the magnetic properties [34, 37]. The magnetic moments of the graphene-like flake embedded h-BN monolayer can be controlled depending on the number of the substituted C atoms in the h-BN monolayers (Figure 4), where α and β are the numbers of the B atoms and the N atoms replaced with the C atoms and positive and negative $(\alpha - \beta)$ values are used for the T1-$C_\alpha C_\beta$ and T2-$C_\alpha C_\beta$ structures, respectively. T1-$C_\alpha C_\beta$ and T2-$C_\alpha C_\beta$ structures give rise to $|\alpha - \beta|\mu_B$ magnetic moments per unit cell. By tuning the sizes of the triangle graphene flakes, the magnetic moments of T1- and T2-graphene-embedded BN sheet are controllable.

The energy band gap values of h-BN monolayers are shown to be tunable [37–39]. By replacing B and N atoms with graphene quantum dots (QD), the energy band gaps of h-BN monolayers decrease. As the size d of the graphene QD increases, it was shown that the band gaps diminish from ~3.6 eV to ~1.6 eV (Figure 5).

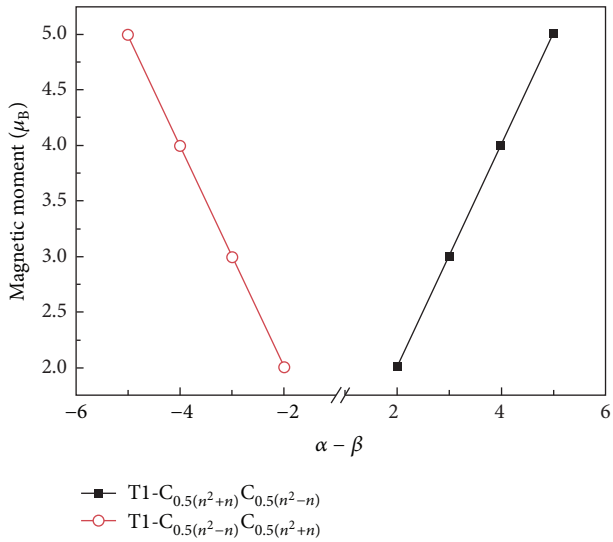

FIGURE 4: Variation of magnetic moments of T1-$C_\alpha C_\beta$ and T2-$C_\alpha C_\beta$ with $(\alpha - \beta)$. Reproduced with permission from [37]; copyright 2011, the American Physical Society.

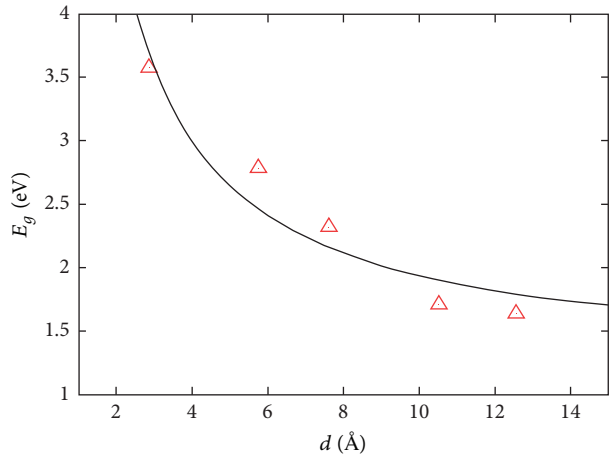

FIGURE 5: Energy band gap value E_g as a function of QD diameter d. Reproduced with permission from [38]; copyright 2011, the American Institute of Physics.

5. Concluding Remarks

We have reviewed the recent works of the first-principles density-functional study of *h*-BN atomic layers. The atomic vacancies can be created in the *h*-BN layers by electron beam irradiation techniques. The triangular-shaped atomic vacancies in *h*-BN layers can give rise to the magnetic moment depending on the vacancy sizes, and moreover the magnetic moment is shown to be tunable under strain.

The C atom can be doped to the *h*-BN layers by using electron beam irradiation combined with introducing the hydrocarbon molecules, and it is deduced that C atoms are doped more easily at B atom sites than at N atom sites. The first-principles density-functional calculations have revealed that the substitution of B atoms with C atoms becomes more favorable in energy than that of N atoms under N-rich conditions. The substitutions of the B atom and the N atom with the C atom induce the donor-like state below the CBM and the acceptor-like state above the VBM, respectively. The ionization energies are controllable for the donor and the acceptor states by applying strain, and furthermore the exotic electronic state can be opened as an active conduction channel under strain.

The graphene-like flake in the *h*-BN layers can modify the magnetic and the electronic properties. By substituting B atoms and N atoms at the two different sublattices with C atoms, the magnetic moment of the *h*-BN layers can be tuned. In addition, the variation of the size of the QD can tune the energy band gaps.

By tuning not only the sizes of the atomic vacancies and the C atoms flake but also strains, new magnetic and electronic properties of the *h*-BN layers would emerge, which might provide the novel nanoelectronics, optoelectronics, and spintronics devices.

Conflicts of Interest

The author declares that there are no conflicts of interest regarding the publication of this paper.

Acknowledgments

This work was partly supported by MEXT Elements Strategy Initiative to Form Core Research Center through Tokodai Institute for Element Strategy and JSPS KAKENHI (Grants nos. JP17K05053 and JP26390062). Computations were partly done at Institute for Solid State Physics, the University of Tokyo, and at Cybermedia Center of Osaka University.

References

[1] K. S. Novoselov, A. K. Geim, S. V. Morozov et al., "Electric field in atomically thin carbon films," *Science*, vol. 306, no. 5696, pp. 666–669, 2004.

[2] A. K. Geim and K. S. Novoselov, "The rise of graphene," *Nature Materials*, vol. 6, no. 3, pp. 183–191, 2007.

[3] C. Berger, Z. Song, X. Li et al., "Electronic confinement and coherence in patterned epitaxial graphene," *Science*, vol. 302, pp. 1191–1196, 2006.

[4] E. V. Castro, K. S. Novoselov, S. V. Morozov et al., "Biased bilayer graphene: semiconductor with a gap tunable by the electric field effect," *Physical Review Letters*, vol. 99, no. 21, Article ID 216802, 2007.

[5] Y. Zhang, Y.-W. Tan, H. L. Stormer, and P. Kim, "Experimental observation of the quantum Hall effect and Berry's phase in graphene," *Nature*, vol. 438, no. 7065, pp. 201–204, 2005.

[6] Y. Zhang, T.-T. Tang, C. Girit et al., "Direct observation of a widely tunable bandgap in bilayer graphene," *Nature*, vol. 459, no. 7248, pp. 820–823, 2009.

[7] J. R. Williams, L. DiCalro, and C. M. Marcus, "Quantum hall effect in a gate-controlled *p-n* junction of graphene," *Science*, vol. 317, no. 5838, pp. 638–641, 2007.

[8] A. F. Young and P. Kim, "Quantum interference and Klein tunnelling in graphene heterojunctions," *Nature Physics*, vol. 5, pp. 222–226, 2009.

[9] D. Pacile, J. C. Meyer, C. O. Girit, and A. Zettl, "In-line phase-contrast imaging of a biological specimen using a compact laser-Compton scattering-based x-ray source," *Applied Physics Letters*, vol. 92, no. 13, Article ID 133107, 2008.

[10] C. Jin, F. Lin, K. Suenaga, and S. Iijima, "Fabrication of a Freestanding Boron Nitride Single Layer and Its Defect Assignments," *Physical Review Letters*, vol. 102, no. 19, 2009.

[11] C. R. Dean, A. F. Young, I. Meric et al., "Boron nitride substrates for high-quality graphene electronics," *Nature Nanotechnology*, vol. 5, no. 10, pp. 722–726, 2010.

[12] N. H. Shon and T. Ando, "Quantum Transport in Two-Dimensional Graphite System," *Journal of the Physical Society of Japan*, vol. 67, pp. 2421–2429, 1998.

[13] K. Watanabe, T. Taniguchi, and H. Kanda, "Direct-bandgap properties and evidence for ultraviolet lasing of hexagonal boron nitride single crystal," *Nature Materials*, vol. 3, pp. 404–409, 2004.

[14] L. Song, L. Ci, H. Lu et al., "Large scale growth and characterization of atomic hexagonal boron nitride layers," *Nano Letters*, vol. 10, no. 8, pp. 3209–3215, 2010.

[15] X. Blase, A. Rubio, S. G. Louie, and M. L. Cohen, "Quasiparticle band structure of bulk hexagonal boron nitride and related systems," *Physical Review B*, vol. 51, no. 11, pp. 6868–6875, 1995.

[16] Y. Kubota, K. Watanabe, O. Tsuda, and T. Taniguchi, "Deep ultraviolet light-emitting hexagonal boron nitride synthesized at atmospheric pressure," *Science*, vol. 317, no. 5840, pp. 932–934, 2007.

[17] K. Watanabe, T. Taniguchi, T. Niiyama, K. Miya, and M. Taniguchi, "Far-ultraviolet plane-emission handheld device based on hexagonal boron nitride," *Nature Photonics*, vol. 3, no. 10, pp. 591–594, 2009.

[18] B. Huang, X. K. Cao, H. X. Jiang, J. Y. Lin, and S. H. Wei, "Origin of the significantly enhanced optical transitions in layered boron nitride," *Physical Review B*, vol. 86, Article ID 155202, 2012.

[19] Y. Fujimoto and S. Saito, "Band engineering and relative stabilities of hexagonal boron nitride bilayers under biaxial strain," *Physical Review B*, vol. 94, Article ID 245427, 2016.

[20] R. Dahal, J. Li, S. Majety et al., "Epitaxially grown semiconducting hexagonal boron nitride as a deep ultraviolet photonic material," *Applied Physics Letters*, vol. 98, no. 21, Article ID 211110, 2011.

[21] S. Majety, J. Li, X. K. Cao et al., "Epitaxial growth and demonstration of hexagonal BN/AlGaN *p-n* junctions for deep ultraviolet photonics," *Applied Physics Letters*, vol. 100, no. 6, Article ID 061121, 2012.

[22] T. Sugino, K. Tanioka, S. Kawasaki, and J. Shirafuji, "Characterization and field emission of sulfur-doped boron nitride synthesized by plasma-assisted chemical vapor deposition," *Japanese Journal of Applied Physics*, vol. 36, part 2, p. L463, 1997.

[23] J. Li, S. Majety, R. Dahal, W. P. Zhao, J. Y. Lin, and H. X. Jiang, "Dielectric strength, optical absorption, and deep ultraviolet detectors of hexagonal boron nitride epilayers," *Applied Physics Letters*, vol. 101, no. 17, Article ID 171112, 2012.

[24] E. Machado-Charry, P. Boulanger, L. Genovese, N. Mousseau, and P. Pochet, "Tunable magnetic states in hexagonal boron nitride sheets," *Applied Physics Letters*, vol. 101, no. 13, Article ID 132405, 2012.

[25] J. C. Meyer, A. Chuvilin, G. Algara-Siller, J. Biskupek, and U. Kaiser, "Selective sputtering and atomic resolution imaging of atomically thin boron nitride membranes," *Nano Letters*, vol. 9, no. 7, pp. 2683–2689, 2009.

[26] J. Kotakoski, C. H. Jin, O. Lehtinen, K. Suenaga, and A. V. Krasheninnikov, "Electron knock-on damage in hexagonal boron nitride monolayers," *Physical Review B—Condensed Matter and Materials Physics*, vol. 82, no. 11, Article ID 113404, 2010.

[27] N. Alem, R. Erni, C. Kisielowski, M. D. Rossell, W. Gannett, and A. Zettl, "Atomically thin hexagonal boron nitride probed by ultrahigh-resolution transmission electron microscopy," *Physical Review B—Condensed Matter and Materials Physics*, vol. 80, no. 15, Article ID 155425, 2009.

[28] Y. Fujimoto and S. Saito, "Energetics and electronic structures of pyridine-type defects in nitrogen-doped carbon nanotubes," *Physica E*, vol. 43, no. 3, pp. 677–680, 2011.

[29] Y. Fujimoto and S. Saito, "Structure and stability of hydrogen atom adsorbed on nitrogen-doped carbon nanotubes," *Journal of Physics: Conference Series*, vol. 302, no. 1, Article ID 012006, 2011.

[30] Y. Fujimoto and S. Saito, "Hydrogen adsorption and anomalous electronic properties of nitrogen-doped graphene," *Journal of Applied Physics*, vol. 115, no. 15, Article ID 153701, 2014.

[31] O. L. Krivanek, M. F. Chisholm, V. Nicolosi et al., "Atom-by-atom structural and chemical analysis by annular dark-field electron microscopy," *Nature*, vol. 464, no. 7288, pp. 571–574, 2010.

[32] X. Wei, M.-S. Wang, Y. Bando, and D. Golberg, "Electron-beam-induced substitutional carbon doping of boron nitride nanosheets, nanoribbons, and nanotubes," *ACS Nano*, vol. 5, no. 4, pp. 2916–2922, 2011.

[33] X. Wei, M.-S. Wang, Y. Bando, and D. Golberg, "Post-synthesis carbon doping of individual multiwalled boron nitride nanotubes via electron-beam irradiation," *Journal of the American Chemical Society*, vol. 132, no. 39, pp. 13592-13593, 2010.

[34] N. Berseneva, A. V. Krasheninnikov, and R. M. Nieminen, "Berseneva, Krasheninnikov, and Nieminen reply:," *Physical Review Letters*, vol. 107, no. 23, Article ID 239602, 2011.

[35] N. Berseneva, A. Gulans, A. V. Krasheninnikov, and R. M. Nieminen, "Electronic structure of boron nitride sheets doped with carbon from first-principles calculations," *Physical Review B—Condensed Matter and Materials Physics*, vol. 87, no. 3, Article ID 035404, 2013.

[36] J. Zhou, Q. Wang, Q. Sun, and P. Jena, "Electronic and magnetic properties of a BN sheet decorated with hydrogen and fluorine," *Physical Review B*, vol. 81, Article ID 085442, 2010.

[37] M. Kan, J. Zhou, Q. Wang, Q. Sun, and P. Jena, "Tuning the band gap and magnetic properties of BN sheets impregnated with graphene flakes," *Physical Review B*, vol. 84, no. 20, Article ID 205412, 2011.

[38] J. Li and V. B. Shenoy, "Graphene quantum dots embedded in hexagonal boron nitride sheets," *Applied Physics Letters*, vol. 98, no. 1, Article ID 013105, 2011.

[39] A. Ramasubramaniam and D. Naveh, "Carrier-induced antiferromagnet of graphene islands embedded in hexagonal boron nitride," *Physical Review B*, vol. 84, no. 7, Article ID 075405, 2011.

[40] L. Ci, L. Song, C. Jin et al., "Atomic layers of hybridized boron nitride and graphene domains," *Nature Materials*, vol. 9, no. 5, pp. 430–435, 2010.

[41] Y. Fujimoto and S. Saito, "Effects of strain on carbon donors and acceptors in hexagonal boron nitride monolayers," *Physical Review B*, vol. 93, Article ID 045402, 2016.

[42] Y. Fujimoto and K. Hirose, "First-principles treatments of electron transport properties for nanoscale junctions," *Physical Review B*, vol. 67, Article ID 195315, 2004.

[43] Y. Fujimoto, K. Hirose, and T. Ohno, "Calculations of surface electronic structures by the overbridging boundary-matching method," *Surface Science*, vol. 586, no. 1–3, pp. 74–82, 2005.

[44] Y. Fujimoto and K. Hirose, "First-principles calculation method of electron-transport properties of metallic nanowires," *Nanotechnology*, vol. 14, no. 2, pp. 147–151, 2003.

[45] Y. Fujimoto, Y. Asari, H. Kondo, J. Nara, and T. Ohno, "First-principles study of transport properties of Al wires: Comparison between crystalline and jellium electrodes," *Physical Review B*, vol. 72, no. 11, Article ID 113407, 2005.

[46] T. Ono, S. Tsukamoto, Y. Egami, and Y. Fujimoto, "Real-space calculations for electron transport properties of nanostructures," *Journal of Physics: Condensed Matter*, vol. 23, no. 39, Article ID 394203, 2011.

[47] A. J. Du, Y. Chen, Z. Zhu, R. Amal, G. Q. Lu, and S. C. Smith, "Dots versus antidots: computational exploration of structure, magnetism, and half-metallicity in boron-nitride nanostructures," *Journal of the American Chemical Society*, vol. 131, no. 47, pp. 17354–17359, 2009.

[48] H.-X. Yang, M. Chshiev, D. W. Boukhvalov, X. Waintal, and S. Roche, "Inducing and optimizing magnetism in graphene nanomeshes," *Physical Review B - Condensed Matter and Materials Physics*, vol. 84, no. 21, Article ID 214404, 2011.

[49] E. H. Lieb, "Two theorems on the Hubbard model," *Physical Review Letters*, vol. 62, no. 10, pp. 1201–1204, 1989.

[50] Y. Fujimoto, T. Koretsune, S. Saito, T. Miyake, and A. Oshiyama, "A new crystalline phase of four-fold coordinated silicon and germanium," *New Journal of Physics*, vol. 10, Article ID 083001, 2008.

[51] Y. Fujimoto and A. Oshiyama, "Formation and Stability of 90 Degree Dislocation Cores in Ge Films on Si(001)," *AIP Conference Proceedings*, vol. 1399, no. 1, p. 185, 2011.

[52] Y. Fujimoto and S. Saito, "Atomic geometries and electronic structures of hexagonal boron-nitride bilayers under strain," *Journal of the Ceramic Society of Japan*, vol. 123, no. 1439, pp. 576–578, 2015.

[53] Y. Fujimoto and S. Saito, "Interlayer distances and band-gap tuning of hexagonal boron-nitride bilayers," *Journal of the Ceramic Society of Japan*, vol. 124, no. 5, pp. 584–586, 2016.

[54] Y. Fujimoto, T. Koretsune, and S. Saito, "Electronic structures of hexagonal boron-nitride monolayer: strain-induced effects," *Journal of the Ceramic Society of Japan*, vol. 122, no. 1425, pp. 346–348, 2014.

[55] J. Tersoff and D. R. Hamann, "Theory and application for the scanning tunneling microscope," *Physical Review Letters*, vol. 50, no. 25, pp. 1998–2001, 1983.

[56] J. Tersoff and D. R. Hamann, "Theory of the scanning tunneling microscope," *Physical Review B*, vol. 31, Article ID 805, 1985.

[57] Y. Fujimoto, H. Okada, K. Endo, T. Ono, S. Tsukamoto, and K. Hirose, "Images of scanning tunneling microscopy on the Si(001)-p(2×2) reconstructed surface," *Materials Transactions*, vol. 42, no. 11, pp. 2247–2252, 2001.

[58] H. Okada, Y. Fujimoto, K. Endo, K. Hirose, and Y. Mori, "Detailed analysis of scanning tunneling microscopy images of the Si(001) reconstructed surface with buckled dimers," *Physical Review B*, vol. 63, no. 19, Article ID 195324, 2001.

[59] Y. Fujimoto and A. Oshiyama, "Structural stability and scanning tunneling microscopy images of strained Ge films on Si(001)," *Physical Review B*, vol. 87, Article ID 075323, 2013.

[60] Y. Fujimoto, H. Okada, K. Inagaki, H. Goto, K. Endo, and K. Hirose, "Theoretical study on the scanning tunneling microscopy image of Cl-Adsorbed Si(001)," *Japanese Journal of Applied Physics*, vol. 42, part 1, no. 8, p. 5267, 2003.

[61] Y. Fujimoto and A. Oshiyama, "Atomic structures and energetics of 90◦ dislocation cores in Ge films on Si(001)," *Physical Review B*, vol. 81, Article ID 205309, 2010.

[62] L. Zhao, M. Levendorf, S. Goncher et al., "Local atomic and electronic structure of boron chemical doping in monolayer graphene," *Nano Letters*, vol. 13, no. 10, pp. 4659–4665, 2013.

[63] Y. Fujimoto and S. Saito, "Energetics and scanning tunneling microscopy images of B and N defects in Graphene Bilayer," *Springer Proceedings in Physics*, vol. 186, pp. 107–112, 2017.

[64] Y. Fujimoto and S. Saito, "Formation, stabilities, and electronic properties of nitrogen defects in graphene," *Physical Review B*, vol. 84, Article ID 245446, 2011.

[65] Y. Fujimoto and S. Saito, "Gas adsorption, energetics and electronic properties of boron- and nitrogen-doped bilayer graphenes," *Chemical Physics*, vol. 478, pp. 55–61, 2016.

[66] Y. Fujimoto and S. Saito, "Electronic structures and stabilities of bilayer graphene doped with boron and nitrogen," *Surface Science*, vol. 634, pp. 57–61, 2015.